



## Equilibrium, kinetic and thermodynamic studies on the adsorption of thiocyanate by steel slag in an aqueous system

Yogesh Nathuji Dhoble<sup>\*1</sup>, Sirajuddin Ahmed<sup>2</sup>

<sup>1</sup>Research Scholar, Jamia Millia Islamia (Central University), New Delhi, India

<sup>2</sup>Professor, Jamia Millia Islamia (Central University), New Delhi, India

### ARTICLE INFO

#### Article history:

Received 21 December 2017

Received in revised form

24 May 2018

Accepted 26 May 2018

#### Keywords:

Adsorption

Isotherms

Kinetics

Steel slag

Thermodynamics

Thiocyanate

Factorial

### ABSTRACT

The use of steel slag in an adsorption process for the removal of thiocyanate has been studied for the first time. Steel slag, a readily available by-product of the steel industry, can be a suitable candidate for the study of the adsorption of thiocyanate found in coke oven effluent. The parameters considered for adsorption studies were pH, initial concentration, temperature, and the amount of adsorbent. It was found that the percentage removal of thiocyanate decreased with an increase in the initial concentration of thiocyanate. The rate of adsorption of thiocyanate increased with an increase in temperature. The adsorption process was spontaneous and exothermic in nature. The Langmuir isotherm was found to be the best fit for the adsorption process. The kinetic data follows the pseudo-second-order model. Main effect and interaction studies were done using the fractional factorial method. The FTIR studies confirmed that functional groups participated in the adsorption process. This made the steel slag a suitable adsorbent for the removal of thiocyanate.

### 1. Introduction

Thiocyanate is found in the wastewater from the coking of coal, quinine factories, base metal mills and gold mines. The salts of thiocyanate like potassium, ammonium, and sodium are used as herbicides. Thiocyanate is considered less toxic; however, its adverse effects on the growth and reproductive system of fish are widely reported [1]. Several industries convert the cyanide present in the effluent into thiocyanate. Thiocyanate is more stable than cyanide, which makes its treatment even more difficult [2]. Several technologies are available for the treatment of thiocyanate. A sequential batch reactor (SBR) is able to remove about 98% of the thiocyanate [3,4]. However, the higher loading of thiocyanate in the SBR severely affects its removal [5]. The four-stage across-the-flow rotating biological contactor (RBC) reactor for the treatment of synthetic wastewater containing phenol and thiocyanate has been studied. It was found that phenol degrades first, then thiocyanate. Firstly, phenol was degraded by bacteria such as *Pseudomonas putida*, *Candida tropicalis* and *Pseudomonas stutzeri* while

thiocyanate degraded at the latter stage in the presence of bacteria like *Thiobacillus thioparus* and *Nocardia* sp. [6]. It was observed that a mixed culture of microorganisms was able to metabolize thiocyanate efficiently [7,8]. Adsorption is an alternative treatment method best suited for the tertiary treatment of wastewater [9]. Studies have reported that thiocyanate removal is affected by pH and phenol as well as ammonia. The removal of thiocyanate is affected by the presence of free ammonia and specific pH conditions [10,11]. However, the removal of thiocyanate is not significantly affected by the presence of phenol [12,13]. Thiocyanate removal is found to increase with the interfering ions in the following order when adsorbed on calcined hydrotalcite: phosphate > sulphate > Chloride > nitrate [14]. Adsorbents such as calcined hydrotalcite [15], surfactant-modified coir pith [16], Fe(III)/Cr(III) hydroxide waste [17], anion exchange resin [18], and AgCl nanoparticles-loaded hydrotalcite [19] are used for the removal of thiocyanate compounds. Most studies report that the adsorption process follows the pseudo-second order model and Langmuir isotherm. This study used steel

\*Corresponding author. Telephone: + 918467888993

E-mail address: [yogeshdhoble@gmail.com](mailto:yogeshdhoble@gmail.com)

DOI: 10.22104/AET.2018.2670.1133

slag as an adsorbent. Very few studies are available on the use of industrial solid waste as an adsorbent [20]. Steel slag is used in the following ways: antiskid aggregate, ceramic ingredient, bituminous mixes, cement ingredient, concrete aggregate, railroad ballast, thermal insulator, landfill daily cover material, sand capping, obtaining calcium carbonate and for carbon sequestration; thus, its commercial value has increased [21]. The novelty of this study is the use of steel slag for the adsorption of thiocyanate. The aim of the present study is to investigate the adsorption characteristics of steel slag while taking into account the equilibrium, kinetic and thermodynamic aspects. The Langmuir and Freundlich isotherms are applied to describe and predict the adsorption equilibrium. Kinetic models including pseudo-first-order equation and pseudo-second-order equation are used to determine the mechanism of adsorption. The intra-particle diffusion model is used to describe the diffusion steps. Thermodynamic parameters such as standard free energy, enthalpy and entropy are also evaluated. The interaction plot and main effect plot provide an understanding of the effect of the parameters. The slag is characterized after and before adsorption by IR studies.

## 2. Materials and methods

Steel slag was obtained from the Steel Authority of India Limited (SAIL), Bokaro, India. It is low cost and an abundantly produced waste material of steel industries. The crushing of steel slag was not required as it was the desired size. For experimental purposes, 150 microns was selected for the slag on the mesh. The size selected was washed with distilled water and dried in an oven at 150°C for 24 hours. It was then kept in a desiccator for further use. The washing and drying steps helped in removing the soluble and other impurities from the steel slag, making the adsorption sites available for the removal of thiocyanate. All the necessary chemicals used in this study were of analytical grade. The standard thiocyanate stock solution was prepared by dissolving 1 g of AR grade potassium thiocyanate (CDH (P) LTD) in 1000 ml of distilled water. The concentration of thiocyanate was determined by iron (III) and measuring the intense red color [22]. The concentrations of thiocyanate in the treated samples were determined by a UV spectrophotometer (Milton Roy Company (USA), range 340-960 nm). All experiments were performed in triplicate. The pH of the solution was measured with a Japsin (Japsin product India) pH meter. XRF was done by a WDXRF Spectrometer - Bruker S4 PIONEER. The SEM images were obtained from the Zeiss Model: V5:05 (SIGMA). XRD was done via Rigaku Smartlab Guidance CuK $\alpha$  irradiation (1.54 Å, 40 kV, 30 mA) and FTIR was done by Vertex 70, Bruker by making KBr pallets. All experiments were done in batch mode. The experiments investigated the effect of adsorbent doses by adding different dosages of slag ranging from 2 to 30 g/L in a series of 100mL flasks containing thiocyanate solution (1 mg/L) which were agitated for 24 hour at 120

rpm at 30 °C. A plot of  $q_e$  and the percentage removal was plotted on the same axis against the adsorbent dose to obtain the optimum dosage of slag required. To elucidate the effect of pH, the experiments were conducted at different pH values which ranged from 2-12 using either HCl (0.03M) or NaOH (0.03M) solutions; the dosage of slag, concentration of the thiocyanate, agitation time, and temperature were kept constant. The effect of contact time was determined to understand the time required by the adsorption process to reach equilibrium. Further experiments were conducted to see the effect of the initial concentrations of thiocyanate onto the slag under the following conditions: the initial concentrations of thiocyanate was varied in the range of 5- 25 mg/L; an optimum pH, i.e., 4; and an optimum adsorbent slag dosage, i.e., 6.2 g/L. The effect of temperature was studied by varying the temperature: 30, 40 and 50°C. The amount of thiocyanate adsorbed per unit mass of the adsorbent was evaluated by Equation 1 [23].

$$q_e = (C_o - C_t) * v / m \quad (1)$$

The percent removal of thiocyanate was calculated by Equation 2.

$$\% \text{ removal} = ((C_o - C_t) / C_o) * 100 \quad (2)$$

Where,  $C_o$  is the initial concentration of thiocyanate,  $C_t$  is final concentration in mg/L at any time  $t$ ,  $V$  is volume of solution in mL of adsorbate solution and  $m$  is the dose of slag in gram.

### 2.1. Kinetic studies

The adsorption kinetics of thiocyanate is tested using the pseudo-first order, pseudo-second-order. The mechanism of adsorption depends on the physical and chemical characteristics of the adsorbent as well as on the mass transfer process. The compliance between experimental data and the model predicted values is expressed by correlation coefficients ( $R^2$ ) to determine the best suitable kinetic model. Lagergren proposed the pseudo-first order kinetic model; its integrated form is given by Equation 3.

$$\text{Log}(q_{eq} - q) = \text{log } q_{eq} - (K_1 / 2.303) * t \quad (3)$$

where  $q$  the amount of thiocyanate adsorbed at time  $t$  (min),  $q_{eq}$  is the amount of thiocyanate adsorbed at equilibrium and  $K_1$  is the rate constant of pseudo-first order adsorption. The values of the adsorption rate constant  $K_1$  for the thiocyanate-Slag system is determined from the plot of  $\text{Log } (q_{eq} - q)$  against  $t$ . The adsorption kinetic can also be given by a pseudo-second order reaction, and its integrated linearized form is given by Equation 4.

$$t/q = 1/k_2 q_{eq}^2 + 1/q_{eq} * t \quad (4)$$

where  $k_2$  the pseudo-second order is the rate constant of the thiocyanate adsorption. The plot of  $t/q$  versus  $t$  of the above equation will give a linear relationship, from which

$q_{eq}$  and  $K_2$  can be determined. The effect of temperature on the rate constant can be seen from the Arrhenius equation as given in Equation 5.

$$K_{ad} = A e^{-E_a/RT} \quad (5)$$

where  $E_a$  (KJ/mole) is the activation energy which is the minimum amount of energy required to initiate a chemical adsorption.  $T$  is the temperature in Kelvin,  $K_{ad}$  is the adsorption rate constant and  $R$  is  $8.314 \text{ J K}^{-1} \text{ mol}^{-1}$ . The intra-particle diffusion model in its linearized form is shown in Equation 6 [24]. It suggests that when a plot of  $q_t$  versus  $t^{0.5}$  is linear and passes through the origin, then intra-particle diffusion is the rate-controlling step or else it indicates some degree of boundary layer control.

$$q_t = K_i t^{0.5} + C \quad (6)$$

where  $C$  is the intercept and  $K_i$  is the intra-particle diffusion rate constant ( $\text{mg/g min}^{0.5}$ ).

## 2.2. Equilibrium studies

Adsorption equilibrium studies provide information on surface properties and the affinity of the adsorbent for the adsorption equilibrium data of the thiocyanate-slag system. The equilibrium study is done using Langmuir and Freundlich isotherm models. The Langmuir isotherm is valid for monolayer adsorption onto a surface containing a finite number of identical sites. It is the most popular model due to its good agreement with sorption experimental data. The Langmuir equation is given by Equation 7 [25].

$$C_e/q_e = 1/K_L q_m + C_e/q_m \quad (7)$$

where  $K_L$  is the Langmuir adsorption constant related to the energy of adsorption and  $q$ ,  $q_m$  signifies adsorption capacity ( $\text{mg/g}$ ).

The Freundlich isotherm theory [26] is the most widely used and is applicable to adsorption on heterogeneous surfaces. It can be represented in linear form by Equation 8.

$$\log q_e = \log K_f + 1/n \cdot \log C_e \quad (8)$$

where  $K_f$  is the Freundlich constant ( $\text{mg/g}$ ) which indicates the relative adsorption capacity of the adsorbent and  $n$  is the Freundlich exponent which indicates the intensity of adsorption.

## 2.3. Thermodynamic Studies

Thermodynamic studies provide information on spontaneity as well as the exothermic or endothermic nature of the process. The thermodynamics study communicates the feasibility of the process. The standard enthalpy change is estimated by applying the Van't Hoff equation and equilibrium constant [27].

$$\Delta G^\circ_{ad} = -RT \ln K_{ad} \quad (9)$$

$$\Delta G^\circ_{ad} = \Delta H^\circ - T\Delta S^\circ \quad (10)$$

$$\ln K_{ad} = -\Delta H^\circ/RT - \Delta S^\circ/R \quad (11)$$

$$K_{ad} = C_o/C_e \quad (12)$$

where  $\Delta G^\circ_{ad}$  is the free energy change ( $\text{kJ/mol}$ ),  $\Delta H^\circ$  is the standard enthalpy change ( $\text{J/mol}$ ),  $\Delta S^\circ$  is the standard entropy change ( $\text{J/mol K}$ ),  $T$  is the absolute temperature ( $\text{K}$ ),  $K_{ad}$  is the equilibrium constant of interaction between the adsorbate and the slag surface, and  $R$  is the universal gas constant. Main effect and interaction studies are performed to understand the parameters affecting the removal of thiocyanate using fractional factorial experimental design  $2^{4-1}$ . Main effect and interaction studies are very important in understanding the effect of one factor over the other in adsorption studies [28]. Conventional studies fail to reveal the interactions between the factors [29]. Main effect and interaction studies are done using the R statistical tool with a graphical user interface. The size of randomization is done for four factors and two levels. The factors chosen for the study include the dosage of slag, initial concentration of adsorbate, time of adsorption, and pH of the solution. The experiments are repeated thrice. FTIR studies help to understand the surface phenomenon. The chemical structure of the adsorbent can provide vital information concerning the functional groups participating in the adsorption process [30]. FTIR on the slag is done before and after the adsorption of thiocyanate. KBr pellets of a sample are made for the analysis.

## 3. Results and discussion

The standard calibration curve equation of the known concentrations of thiocyanate was  $y = 0.0287x$  of  $R^2 = 0.9987$ , and the maximum absorbance of thiocyanate was  $475 \text{ nm}$ .

### 3.1. Steel slag characterization

The grain size of steel slag can be seen in Figure 1. Sieve analysis shows that the steel slag is well graded. The coefficient of uniformity is 7.5, the coefficient of curvature is 0.5, and the specific gravity is 2.85. The steel slag composition obtained from XRF is  $\text{SiO}_2$  17.23%,  $\text{Al}_2\text{O}_3$  1.15%,  $\text{CaO}$  45%,  $\text{MgO}$  10.12%,  $\text{FeO}$  17% and  $\text{MnO}$  12.42%. The SEM image in Figure 2 shows the porous nature of the steel slag which indicates the abundance of adsorption sites on its surface. The BET surface area is  $11.6 \text{ m}^2/\text{g}$ , the pore diameter is  $4.06 \text{ nm}$  and the pore volume of the slag is  $0.010 \text{ cc/g}$ . The XRD analysis reveals the presence of amorphous silica structure [31],  $\text{Ca(OH)}_2$ ,  $(\text{Mg}.39 \text{ Fe}.52 \text{ Ca}.09) \text{ SiO}_3$  [32],  $\text{C}_2\text{S}$ ,  $\text{C}_3\text{S}$ , Periclase [33], Akermanite [34], and Calcite [35].



Fig. 1. Steelmaking slag sample

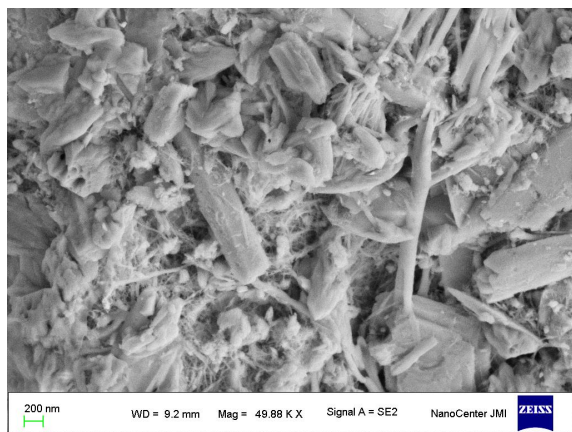


Fig. 2. SEM of steel making slag

### 3.2. Intra-particle Diffusion

The multi-linear nature of the plot can be seen in Figure 3 which suggests that the process of adsorption is controlled by more than one mechanism. The initial phase is steep which represents surface diffusion. The second lesser steep phase represents a gradual adsorption of thiocyanate where intra-particle diffusion within the pores is rate-limiting. The third phase represents achieved equilibrium [36]. Since the line did not pass through the origin, intra-particle diffusion is not the only rate-limiting step. The values of the intra-particle diffusion model constants  $K_i$  is 0.0077. The thickness of the boundary layer ( $C$ ) is 0.0676, which is very small and suggests that surface diffusion plays a smaller role as the rate-limiting step in the overall adsorption process.

### 3.3. Effect of adsorbent dose

The increase in adsorbent dosage increases the percentage removal, indicating the presence of a large surface area available for adsorption. Figure 4 shows that the maximum percentage of thiocyanate removal achieved is 82.57 %. The optimum dosage is considered at the intersection. Therefore, 6.2 g/L is kept as the optimum adsorbent dosage for all experiments.

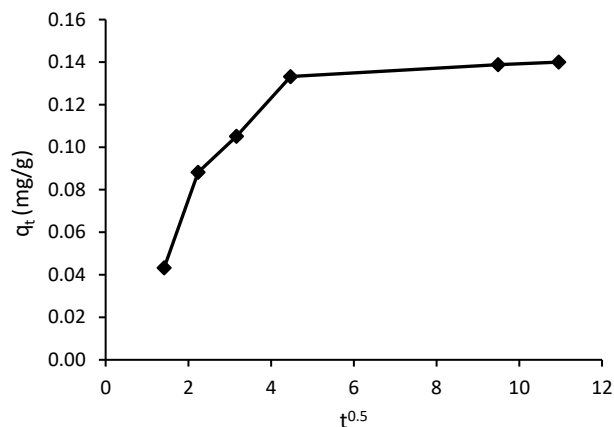


Fig. 3. Intra-particle diffusion model plot

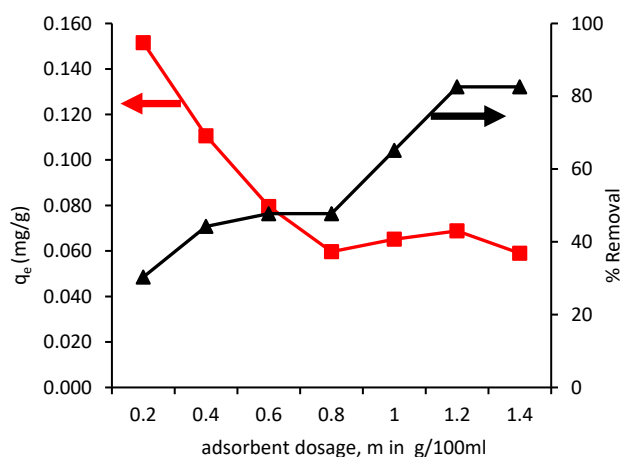


Fig. 4. Effect of adsorbent dose for thiocyanate removal at neutral pH for 250 min at 30°C

### 3.4. Effect of initial pH

The increase in thiocyanate adsorption occurs at pH 4 and decreases as the pH increases. The electrostatic forces between the protonated group of adsorbent and the anionic thiocyanate plays an important role in the process of adsorption. The adsorption of thiocyanate on the slag might be an anionic process [37]. The maximum adsorption is attained at the pH of 4.

### 3.5. Effect of contact time and initial thiocyanate concentration

To observe the effect of contact time and initial concentrations on the adsorption process, a graph is plotted with  $q_e$  versus time and is shown in Figure 5.

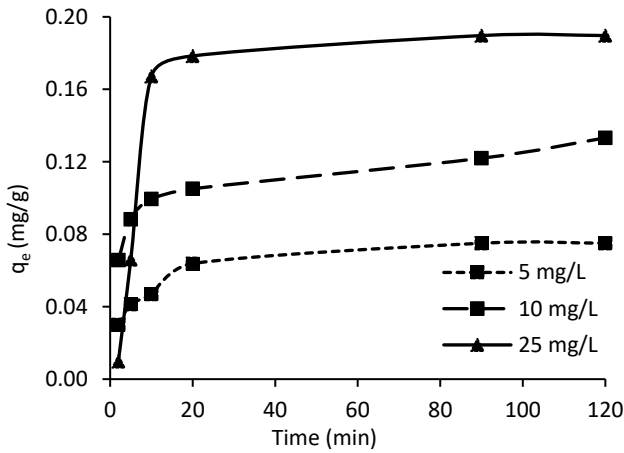


Fig. 5. Effect of contact time and initial conc. on the adsorption of thiocyanate on to slag

In the present study, the equilibrium time required for the adsorption of thiocyanate onto *slag* is 120 minutes. However, the results also indicate that up to 90% of the total amount of thiocyanate uptake occurs in the first 20 min. The percentage adsorption drastically decreases with an increase in initial thiocyanate concentration. For the initial concentration of 5 mg/L, 10 mg/L and 25 mg/L, the percentage removal observed is 93 %, 82.57 %, 37 %, respectively. The adsorption capacity for slag is found to increase with the increase in thiocyanate concentration. The uptake capacity increases with an increase in initial concentration, which may be due to the availability of more thiocyanate ions in the solution for sorption [38].

### 3.6. Effect of Temperature

A plot of the uptake capacity of *slag* against time at different temperatures is shown in Figure 6. It is evident that the value of maximum adsorption capacity  $q_e$  decreases slightly with a decrease in temperature, thus suggesting that adsorption may be favored at higher temperatures. However, the effect of temperature is found to be insignificant for the small range of temperatures studied. An increase in temperature disrupts the hydrogen bonds of the hydration shell helping the thiocyanate group to be adsorbed on the surface of the steel slag [39].

### 3.7. Equilibrium kinetics studies

The values of the adsorption rate constant  $K_1$  for the thiocyanate-*slag* system for the pseudo-first order kinetic

model are determined from Figure 7. The values of  $q_{eq}$  and  $K_2$  of the pseudo-second order reaction are determined from the slope and intercept of the plot which is shown in Figure 8.

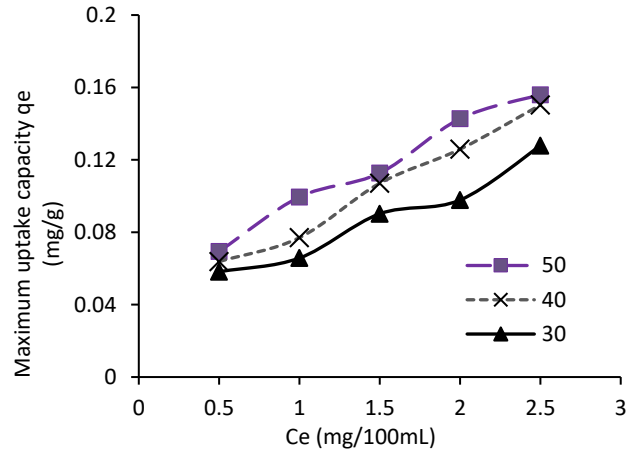


Fig. 6. Effect of temperature for thiocyanate removal (pH 4, t:120 min, m 6.2 g/L)

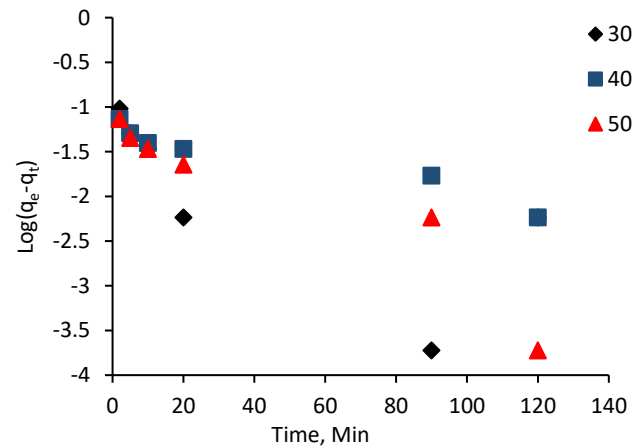


Fig. 7. Pseudo first order kinetic plot ( $C_0 = 10$  mg/L,  $m = 6.2$  g/L)

The correlation coefficient ( $R^2$ ) is greater for the pseudo-second-order model than the pseudo-first-order kinetic model as shown in Table 2. Thus, it can be concluded that the pseudo second order kinetic model provides a good correlation for the adsorption of thiocyanate onto steel slag. This also corroborates with the studies done by other researchers [15-17], [40].

Table 2. Kinetic parameters for the removal of thiocyanate by slag ( $C_0 = 10$  mg/L,  $m = 6.2$  g/L)

	$C_0$	$K_f$	$R^2$
Pseudo-first order kinetic model	30	0.032012	0.5122
	40	0.017273	0.9242
	50	0.040993	0.8908
	$C_0$	$K_s$	$R^2$
Pseudo-second-order model	30	0.376999	0.9983
	40	0.473321	0.9968
	50	0.445572	0.9994

Table 2 shows that the rate of adsorption increases with the increase in the temperature. The activation energy is calculated from Figure 9. The activation energy for the pseudo-first order reaction is 9.41 KJ/mole with  $R^2$  0.0676 which is unacceptable because  $R^2$  is not close to 1. The activation energy for the pseudo-second order reaction is 6.92 KJ/mole with  $R^2$  0.5211. As the activation energy is <40 KJ/mole, the process of adsorption is physisorption [41].

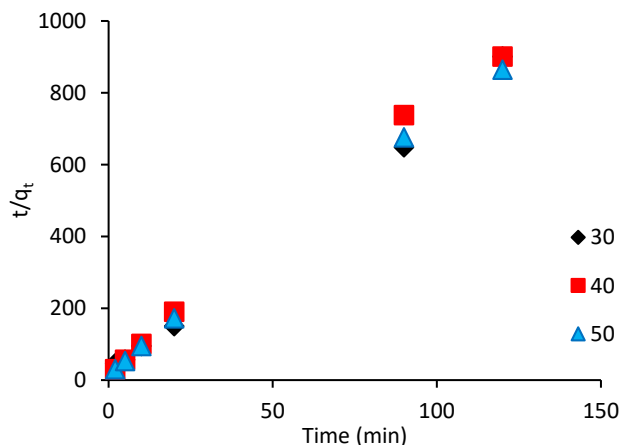


Fig. 8. Pseudo-second-order kinetic plot ( $C_0 = 10$  mg/L,  $m = 6.2$  g/L)

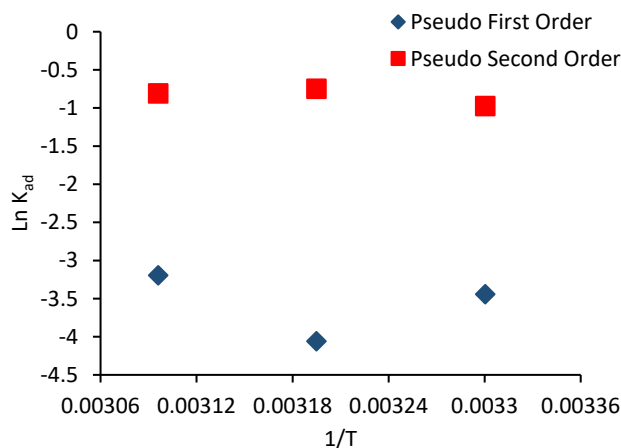


Fig. 9. Activation Energy

### 3.8 Calculation of activation energy

The Freundlich and Langmuir isotherm constants are determined at 30, 40 and 50 °C, and their results are shown in Table 3. The Freundlich constants,  $K_f$  and  $1/n$ , indicate the adsorption capacity and adsorption intensity, respectively. The higher the value of  $1/n$ , the higher the affinity between the adsorbate and adsorbent as well as the heterogeneity of the adsorbent sites. The  $1/n$  value indicates the relative distribution of energy sites and depends on the nature and strength of the adsorption process. For example,  $1/n = 0.25$  to  $0.38$  refers to the fact that 25 to 38 % of the active

adsorption sites have an equal energy level. Since  $1/n < 1$ , thiocyanate is favorably adsorbed by slag at all temperatures. The surface heterogeneity is due to the existence of crystal edges, type of cations, and surface charges. The magnitude of  $K_f$  also shows the lower uptake of thiocyanate at higher temperatures indicating the exothermic nature of the adsorption process. The data in Table indicates that the values of  $q_m$  decrease with an increase in temperature, confirming the exothermic nature of the overall sorption process. Overall, the analysis of the equilibrium model indicates the fitness of the Langmuir model [15-18], [40]. The maximum sorption capacity of steel slag for thiocyanate is 0.14 mg/g at 30 °C.

### 3.9. Thermodynamics study

The values of  $\Delta G$ ,  $\Delta H$ ,  $\Delta S$  obtained from Equation 10 to 13 are shown in Table 4. The value of  $\Delta H^\circ$  for thiocyanate slag adsorption systems at 30 °C and 10 mg/L were -0.018 J/mol. The values of  $\Delta S^\circ$  for the respective systems were 0.051 J/mol K under the same conditions, indicating that the adsorption process was spontaneous in nature. The positive value of  $\Delta S^\circ$  suggested an increased randomness at the solid-solution interface and an increase in the degree of freedom of the adsorbed species. The negative value of  $\Delta H$  also suggested that the adsorption process was exothermic in nature.

Table 3. Isotherm parameters and regression coefficient for the removal of thiocyanate by slag

Freundlich			
Temp.(°C)	Log $K_f$	$1/n$	$R^2$
30	1.031	0.384	0.807
40	0.936	0.304	0.860
50	0.879	0.254	0.954
Langmuir			
Temp. (°C)	$q$ (mg/g)	$K$ (l/mg)	$R^2$
30	0.142	2.219	0.873
40	0.175	2.364	0.892
50	0.170	4.478	0.958

Table 4. Thermodynamic results of the batch experiment at different concentration ( $t = 120$  min,  $m = 6.2$  g/L).

Concentration	5 mg/L	10 mg/L	15 mg/L	25 mg/L
$\Delta S$ (J/mol K)	0.077	0.051	0.016	0.025
$\Delta H$ (J/mol)	-0.028	-0.018	-0.006	-0.009
$\Delta G$ (J/mol), 30 °C	-23.344	-15.456	-4.883	-7.573
$\Delta G$ (J/mol), 40 °C	-24.114	-15.966	-5.044	-7.822
$\Delta G$ (J/mol), 50 °C	-24.883	-16.475	-5.205	-8.072

### 3.10. Main effect and Interaction studies

The experimental results for the fractional factorial method are mentioned in Table 5. The type II test of Anova, Table 6, was performed on the results and all the parameters considered for the adsorption process were significant and affected the process of adsorption. It was also observed that the initial concentration has a relationship with dosage, pH and time of contact. The main effect plot, as shown in Figure 10 represents the results of the regression analysis which further explains the parameter effect. It suggests that the process of adsorption of thiocyanate is more dependent on pH, then on initial concentration followed by contact time. The removal of thiocyanate is too sensitive. As the dosage of slag and the initial concentration and pH increase, the percentage removal of thiocyanate decreases. However, an increase in contact time is found to increase the percentage removal. The interaction plot for the four factors, as shown in Figure 11 provides further analysis: a higher dosage and lower initial concentration favors the adsorption process. Similarly, a lower dosage and maximum contact time also provides a better percentage removal, provided the initial concentration is not too high. If the pH of the solution is high even after a lower dosage and providing maximum contact time, the removal efficiency decreases. Therefore, the adsorption of thiocyanate can be termed as too sensitive at a higher pH. The initial concentration is required to be monitored. The removal performance of slag can be improved even in a low dosage of slag.

**Table 5.** Experiments for main effect and interaction plot

Sr no	Dosage	Conc	Time	pH	T.Removal (Avg)	Std.dev
1	1	1	120	12	29.3	0.04
2	16	16	120	12	20.7	2.7
3	1	1	5	2	47	0.87
4	16	16	5	2	15.4	1.25
5	1	16	5	12	15	0.78
6	16	1	5	12	30.2	1.78
7	16	1	120	2	59.1	2.7
8	1	16	120	2	22	0.37
9	8.5	8.5	62.5	7	35	2.5

class=design, type= FrF2.center

**Table 6.** Anova Table (Type II tests)

	Sum Sq	Df	F Value	Pr(>F)
Conc	61815	1	268872.44	0.001228
Dosage	1019	1	4434.02	0.009560
pH	304	1	1320.37	0.017515
Time	477	1	2073.21	.0013979
Conc:Dosage	473	1	1900.78	0.014600
Conc:pH	206	1	897.29	0.021245
Conc:time	299	1	1302.67	0.017634
Dosage:pH	0			
Dosage:time	0			
pH:time	0			
Conc:Dosage:pH	0			
Conc:Dosage:time	0			
Conc:pH:time	0			
Dosage:pH:time	0			
Residuals	0	1		

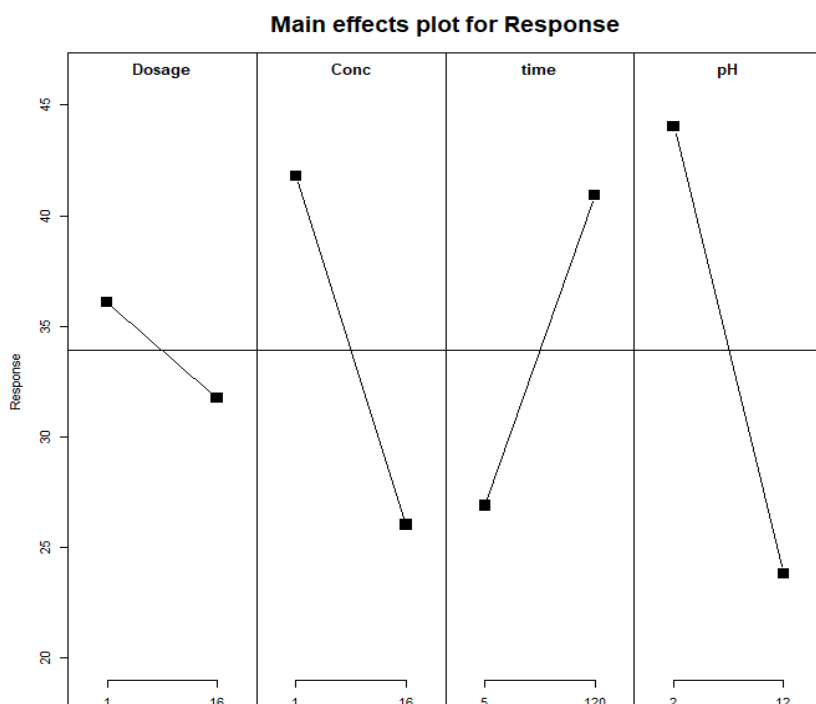


**Fig. 10.** Main effect plot for the removal of thiocyanate

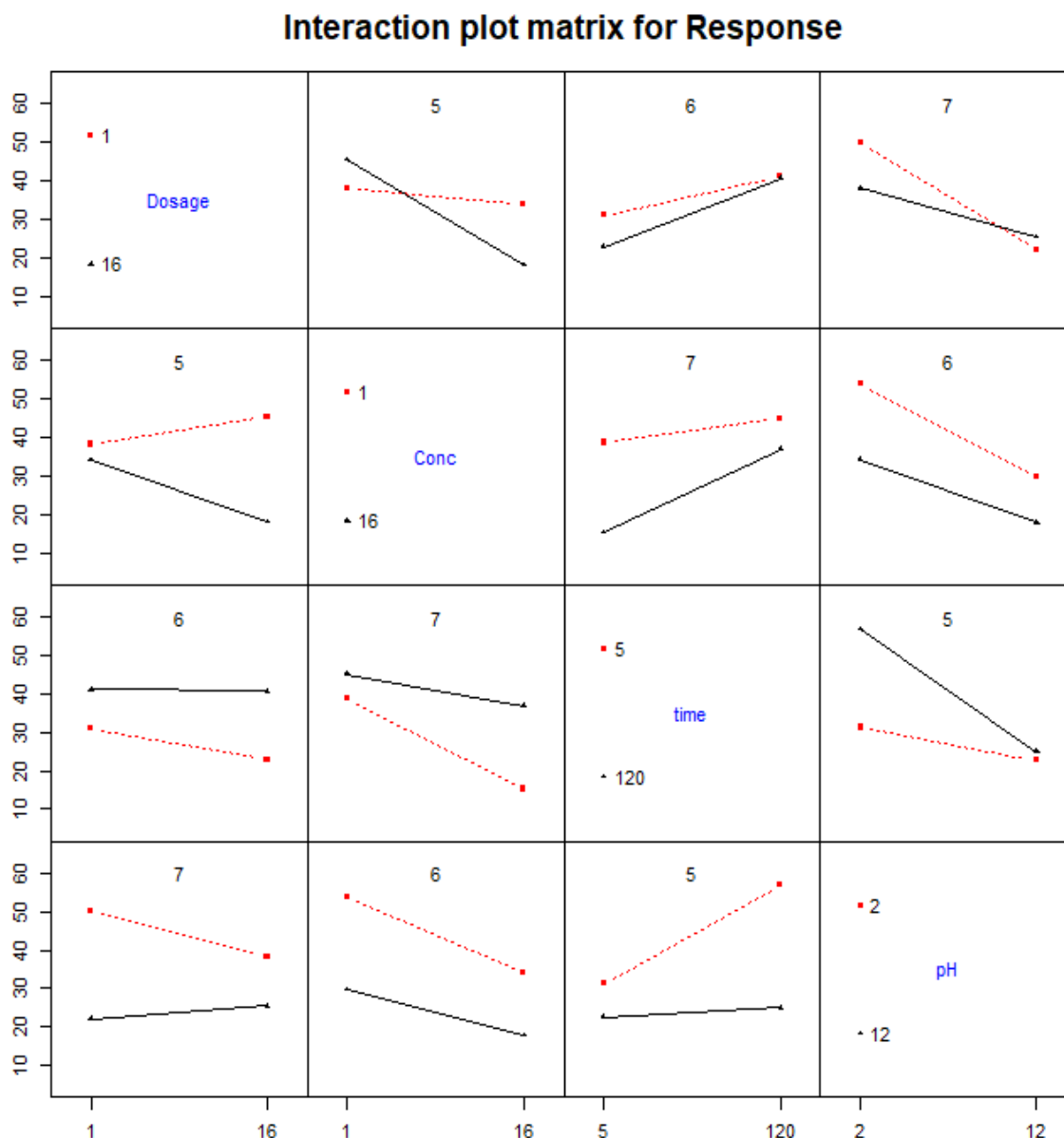


**Fig. 11.** Interaction plot for the removal of thiocyanate

### 3.11. FTIR studies

The FTIR results are shown Figure 12. The periclase (MgO) is found between  $800$  to  $1114\text{ cm}^{-1}$  [42]. The oxides of Fe are found at  $476$  and  $786\text{ cm}^{-1}$  [43]. Vibrational change is observed for -SCN in the range of  $1600$  to  $2250\text{ cm}^{-1}$  for the sample after adsorption with thiocyanate [44-45].

Vibrational changes of high intensity are observed in the band of  $405$  to  $1250\text{ cm}^{-1}$  which shows the participation of oxides of magnesium and iron in the process of adsorption. Medium intensity changes are observed in the band of  $2500$  to  $3000\text{ cm}^{-1}$ . The FTIR studies reveal that functional groups are participating in the process of adsorption.

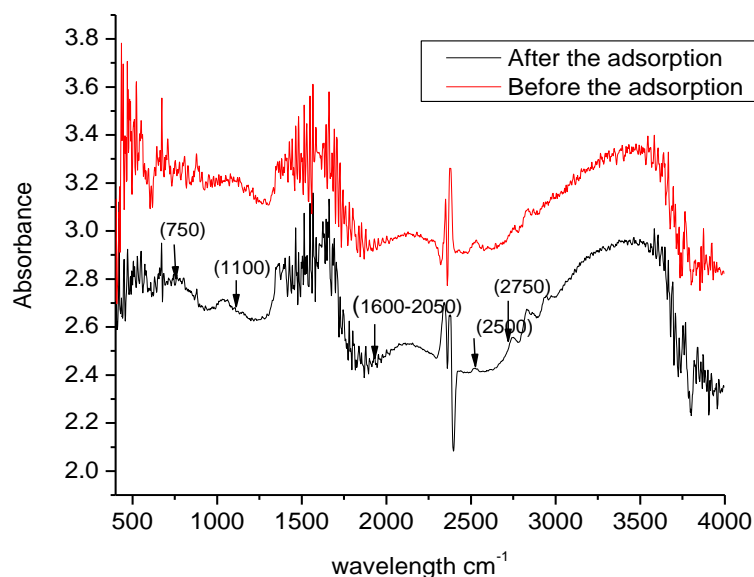


Fig. 12. FTIR studies on the slag before and after adsorption

### 3.12. Regeneration

It is reported that the adsorption capacity of modified steel slag can be regenerated five times by calcining it to 800°C for 120 min and then cooled. It is observed that the efficiency of the modified steel slag is reduced from 35 % to 18 % after the 5<sup>th</sup> regeneration. This shows that steel slag can be regenerated for further adsorption [46]. Since steel slag is an abundantly produced waste material, regenerating it for adsorption would not be economically feasible.

### 4. Conclusions

The maximum uptake of thiocyanate on to steel slag obtained from the Bokaro steel plant was found to be 0.14 mg/g. The optimum conditions for the adsorption of thiocyanate onto steel slag was 120 min, pH of 4 at the initial concentration of 10 mg/L, and a temperature of 30°C. The amount of slag required for adsorption was 6.2 g/L. Up to 82 percent removal of thiocyanate was possible by the steel slag. The overall analysis of the equilibrium model indicated the fitness of the Langmuir model. Kinetics studies indicated that the reaction followed the pseudo-second order rate; the thermodynamic studies revealed that the adsorption was spontaneous and exothermic in nature; also, the rate of adsorption increased with the increase in temperature. It was also concluded that the process of adsorption was mainly dependent on the pH of the slag and initial concentration. The FTIR results indicated that functional groups participated in the process of adsorption. This study revealed that steel slag can be used as a potential adsorbent for the removal of thiocyanate from the aqueous solution. However, due care is required for the optimization

of thiocyanate removal as all the studied parameters are found to significantly affect the removal efficiency.

### Acknowledgement

The authors are thankful to the Department of Nanotechnology, Jamia Millia Islamia, NewDelhi, for providing instrumentation support for the analysis of the sample.

### References

- [1] Bhunia, F., Saha, N. C., Kaviraj, A. (2000). Toxicity of thiocyanate to fish, plankton, worm, and aquatic ecosystem. *Bulletin of environmental contamination and toxicology*, 64(2), 197-204.
- [2] Gould, W. D., King, M., Mohapatra, B. R., Cameron, R. A., Kapoor, A., Koren, D. W. (2012). A critical review on destruction of thiocyanate in mining effluents. *Minerals engineering*, 34, 38-47.
- [3] Sirajuddin, A., Rathi, R. K., Umesh, C. (2010). Wastewater Treatment technologies commonly practiced in major steel industries of India. In *16th annual international sustainable development research conference* (Vol. 30).
- [4] Maranon, E., Vazquez, I., Rodriguez, J., Castrillon, L., Fernandez, Y., Lopez, H. (2008). Treatment of coke wastewater in a sequential batch reactor (SBR) at pilot plant scale. *Bioresource technology*, 99(10), 4192-4198.
- [5] Sirianuntapiboon, S., Chairattanawan, K., Surasinanant, P. (2007). Some properties of a sequencing batch reactor for treatment of wastewater containing thiocyanate compounds. *Journal of environmental management*, 85(2), 330-337.

- [6] Banerjee, G. (1996). Phenol-and thiocyanate-based wastewater treatment in RBC reactor. *Journal of environmental engineering*, 122(10), 941-948.
- [7] Ahmed, S., Popov, V., Trevedi, R. C. (2008, May). Constructed wetland as tertiary treatment for municipal wastewater. In *proceedings of the institution of civil engineers-waste and resource management* (Vol. 161, No. 2, pp. 77-84). Thomas Telford Ltd.
- [8] Souza-Fagundes, E. M., Rosa, L. H., Gomes, N., Santos, M. H., Pimentel, P. F. (2004). Thiocyanate degradation by pure and mixed cultures of microorganisms. *Brazilian journal of microbiology*, 35(4), 333-336.
- [9] Ahmed, S., Dhoble, Y., Gautam, S. (2012). Trends in patenting of technologies related to wastewater treatment.
- [10] Z. Grenoble et al., (2007, October) "Physico-chemical processes," *Water environ. Research*. 79(10), 1228-1296,.
- [11] Lay-Son, M., Drakides, C. (2008). New approach to optimize operational conditions for the biological treatment of a high-strength thiocyanate and ammonium waste: pH as key factor. *Water research*, 42(3), 774-780.
- [12] Dhoble, Y., Ahmed, S. (2017). Removal of Phenol, Ammonia and Thiocyanate Either Alone or in Combination by the Adsorption with Steel Slag. *International. Journal of Engineering Research Developement*, 13(12), 2278-67.
- [13] Staib, C., Lant, P. (2007). Thiocyanate degradation during activated sludge treatment of coke-ovens wastewater. *Biochemical engineering journal*, 34(2), 122-130.
- [14] YANG, M., ZHANG, X. J., WU, T., CAO, N., WEI, N., WANG, J. (2006). Adsorption removal of thiocyanate from aqueous solution by calcined hydrotalcite. *Journal of environmental sciences*, 18(1), 23-28.
- [15] Li, Y., Gao, B., Wu, T., Chen, W., Li, X., Wang, B. (2008). Adsorption kinetics for removal of thiocyanate from aqueous solution by calcined hydrotalcite. *Colloids and surfaces A: physicochemical and engineering aspects*, 325(1-2), 38-43.
- [16] Namasivayam, C., Sureshkumar, M. V. (2007). Modelling thiocyanate adsorption onto surfactant-modified coir pith, an agricultural solid 'waste'. *Process safety and environmental protection*, 85(6), 521-525.
- [17] Namasivayam, C., Prathap, K. (2006). Removal of thiocyanate by industrial solid waste Fe (III)/Cr (III) hydroxide: Kinetic and equilibrium studies. *Journal of environmental engineering and management*, 16(4), 267-274.
- [18] Dizge, N., Demirbas, E., Kobya, M. (2009). Removal of thiocyanate from aqueous solutions by ion exchange. *Journal of hazardous materials*, 166(2-3), 1367-1376.
- [19] Xie, F., Borowiec, J., Zhang, J. (2013). Synthesis of AgCl nanoparticles-loaded hydrotalcite as highly efficient adsorbent for removal of thiocyanate. *Chemical engineering journal*, 223, 584-591.
- [20] R. Ahmad et al., (October 2005) Physico-Chemical Processes, *Water Environmental. Research* 77( 6), 982-1156.
- [21] Das, B., Prakash, S., Reddy, P. S. R., Misra, V. N. (2007). An overview of utilization of slag and sludge from steel industries. *Resources, conservation and recycling*, 50(1), 40-57.
- [22] E. Merck, *Testing of water*. E. Merck, 1974.
- [23] Siva Kumar, N. A. D. A. V. A. L. A., Min, K. (2011). Removal of phenolic compounds from aqueous solutions by biosorption onto *Acacia leucocephala* bark powder: Equilibrium and kinetic studies. *Journal of the Chilean chemical society*, 56(1), 539-545.
- [24] Yakout, S. M., Elsherif, E. (2010). Carbon—science and technology. *Applied science innovations Pvt. Ltd. India*, 1, 144-153.
- [25] Langmuir, I. (1916). The constitution and fundamental properties of solids and liquids. Part I. Solids. *Journal of the American chemical society*, 38(11), 2221-2295.
- [26] Freundlich, H. M. F. (1906). Over the adsorption in solution. *The Journal of Physical Chemistry*, 57(385471), 1100-1107.
- [27] Alzaydien, A. S., Manasreh, W. (2009). Equilibrium, kinetic and thermodynamic studies on the adsorption of phenol onto activated phosphate rock. *International journal of physical sciences*, 4(4), 172-181.
- [28] Bingol, D., Tekin, N., Alkan, M. (2010). Brilliant Yellow dye adsorption onto sepiolite using a full factorial design. *Applied clay science*, 50(3), 315-321.
- [29] Ponnusami, V., Krithika, V., Madhuran, R., Srivastava, S. N. (2007). Biosorption of reactive dye using acid-treated rice husk: factorial design analysis. *Journal of hazardous materials*, 142(1-2), 397-403.
- [30] Daffalla, S. B., Mukhtar, H., Shaharun, M. S. (2010). Characterization of adsorbent developed from rice husk: effect of surface functional group on phenol adsorption.
- [31] Silva, F. G. D., Liborio, J. B., Helene, P. (2008). La mejora de propiedades físicas y químicas de hormigón con sílice de cáscara de arroz (SRH) brasileña. *Revista ingeniería de construcción*, 23(1), 18-25.
- [32] Brown, G. E., Prewitt, C. T., Papike, J. J., & Sueno, S. (1972). A comparison of the structures of low and high pigeonite. *Journal of geophysical research*, 77(29), 5778-5789.
- [33] Jacobsen, S. D., Holl, C. M., Adams, K. A., Fischer, R. A., Martin, E. S., Bina, C. R., Dera, P. (2008). Compression of single-crystal magnesium oxide to 118 GPa and a ruby pressure gauge for helium pressure media. *American mineralogist*, 93(11-12), 1823-1828.
- [34] Kusaka, K., Ohmasa, M., Hagiya, K., Iishi, K., Haga, N. (1998). On variety of the Ca coordination in the incommensurate structure of synthetic iron-bearing

- åkermanite,  $\text{Ca}_2(\text{Mg}_{0.55}, \text{Fe}_{0.45})\text{Si}_2\text{O}_7$ . *Mineralogical journal*, 20(2), 47-58.
- [35] Antao, S. M., Hassan, I. (2010). Temperature dependence of the structural parameters in the transformation of aragonite to calcite, as determined from in situ synchrotron powder X-ray-diffraction data. *The Canadian Mineralogist*, 48(5), 1225-1236.
- [36] Olu-Owolabi, B. I., Diagbaya, P. N., Adebawale, K. O. (2014). Evaluation of pyrene sorption-desorption on tropical soils. *Journal of environmental management*, 137, 1-9.
- [37] Namasivayam, C., Prathap, K. (2006). Removal of thiocyanate by industrial solid waste Fe (III)/Cr (III) hydroxide: Kinetic and equilibrium studies. *Journal of environmental engineering and management*, 16(4), 267-274.
- [38] Srivastava, V. C., Swamy, M. M., Mall, I. D., Prasad, B., Mishra, I. M. (2006). Adsorptive removal of phenol by bagasse fly ash and activated carbon: equilibrium, kinetics and thermodynamics. *Colloids and surfaces a: physicochemical and engineering aspects*, 272(1-2), 89-104.
- [39] Stavropoulos, G. G., Skodras, G. S., Papadimitriou, K. G. (2015). Effect of solution chemistry on cyanide adsorption in activated carbon. *Applied thermal engineering*, 74, 182-185.
- [40] Wu, T., Sun, D., Li, Y., Zhang, H., & Lu, F. (2011). Thiocyanate removal from aqueous solution by a synthetic hydrotalcite sol. *Journal of colloid and interface science*, 355(1), 198-203.
- [41] Inglezakis, V. J., Zorpas, A. A. (2012). Heat of adsorption, adsorption energy and activation energy in adsorption and ion exchange systems. *Desalination and water treatment*, 39(1-3), 149-157.
- [42] Chand, S., Paul, B., Kumar, M. (2016). A comparative study of physicochemical and mineralogical properties of LD Slag from some selected steel plants in India. *Journal of environmental science and technology*, 9(1), 75-87.
- [43] Sharma, G., Pethaiyan, J. (2013). A thermal decomposition approach for the synthesis of iron oxide microspheres. *MRS Online Proceedings library archive*, 1547, 155-160.
- [44] Vu, H. P., Moreau, J. W. (2015). Thiocyanate adsorption on ferrihydrite and its fate during ferrihydrite transformation to hematite and goethite. *Chemosphere*, 119, 987-993.
- [45] Liu, B., Zhang, W., Zhang, Q., Zhang, H., Yu, J., Yang, X. (2012). Facile method for synthesis of hollow porous magnetic microspheres with controllable structure. *Journal of colloid and interface science*, 375(1), 70-77.
- [46] Yang, L., Yang, M., Xu, P., Zhao, X., Bai, H., Li, H. (2017). Characteristics of nitrate removal from aqueous solution by modified steel slag. *Water*, 9(10), 757.